Nitrones as Ligands in Complexes of Cu(II), Mn(II), Co(II), Ni(II), Fe(II), and Fe(III) with *N-tert*-Butyl-α-(2-pyridyl)nitrone and 2,5,5-Trimethyl-1-pyrroline-*N*-oxide†

Frederick A. Villamena, Michael H. Dickman,* and DeLanson R. Crist*

Department of Chemistry, Georgetown University, Washington, DC 20057-2222

Received August 1, 1997

The use of nitrones as ligands was explored by preparing and characterizing complexes of *N-tert*-butyl-α-(2-pyridyl)nitrone (2-PyBN) and 2,5,5-trimethyl-1-pyrroline-*N*-oxide (M_3PO) with Cu(II), Mn(II), Co(II), Ni(II), Fe(II), and Fe(III) hexafluoroacetylacetonates (hfac). Neutral Cu(2-PyBN)$(hfac)_2$, **1**, was formed when equimolar amounts of $Cu(hfac)_2$ and the bidentate 2-PyBN were mixed in methylene chloride. Under the same preparation conditions, an unexpected ligand exchange led to crystalline salts of formula $[M(2\text{-PyBN})_2hfac][M(hfac)_3]$ for M(II) = Mn (**2**), Co (**3**), Ni (**4**), and Fe (**5**) as determined by their X-ray structures. Geometry changes in 2-PyBN on complexation indicate a more localized nitrone C=N bond In **1**−**5**. Crystalline dimers with formulas $[M(M_3PO)(hfac)_2]_2$ for M(II) = Mn (**6**), Co (**7**), and Ni (**8**) were obtained from equimolar solutions of $M(hfac)_2$ and the monodentate M_3PO. The two M(II) ions are bridged by two M_3PO coordinated in a bis, μ-1,1 fashion. With $Fe(hfac)_2$ and M_3PO, however, an apparent air oxidation led to a (μ-oxo)diiron(III) complex $[Fe(M_3PO)(hfac)_2]_2$-(μ-O) (**9**), while with $Zn(hfac)_2$ and *N-tert*-butyl-α-(phenyl-2-pyridyl)nitrone (2PyPhBN) the neutral Zn(2-PyPhBN)$(hfac)_2$ (**10**) was obtained. Results are compared to reported nitronyl nitroxide complexes.

Introduction

Nitrones have numerous applications, such as their use in organic synthesis[1,2] in cycloaddition reactions; as spin-trapping agents[3] due to the stability of resulting nitroxide radicals; and more recently, as possible molecular magnets in the case of nitronyl nitroxide complexes.[4−6] In all these applications metal ions may play an important role, as catalysts in synthesis schemes and in biochemical and radical-generating systems, or by providing desired material science properties.

Surprisingly, only a few complexes of metals with simple nitrones have been reported. These complexes of α-aryl-[7,8] and α-(2-hydroxy-1-naphthyl)nitrones[9] and salicylideneaniline- and naphthylideneaniline-*N*-oxides[10] were characterized by UV, NMR, and IR spectroscopy. The only X-ray structure determinations have involved unusual nitrones such as metallacycles with rhenium[11] and platinum,[12] nitrones bound to transition metal−germylene complexes,[13] a dinitrone with weak interaction to tetrachloroaurate,[14] and metal complexes with a nitrone function as part of a porphyrin[15] or in combination with a complexing nitroxyl group.[5,6]

We now report X-ray structure determinations of complexes of Cu(II), Mn(II), Co(II), Ni(II), Fe(II), and Fe(III) with two simple nitrones chosen because of their structural disimilarity and importance to spin-trapping applications of nitrones. One, *N-tert*-butyl-α-(2-pyridyl)nitrone (2-PyBN), is an analogue of the widely used spin trap *N-tert*-butyl-α-phenylnitrone (PBN) but contains a chelating pyridyl group to enhance complexation. The other, 2,5,5-trimethyl-1-pyrroline-*N*-oxide (M_3PO), is a well-known spin trap.

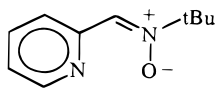

2-PyBN

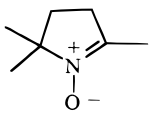

M_3PO

Experimental Section

Materials and Reagents. $Fe(hfac)_2$ was prepared by dissolving 0.010 g (0.48 mmol) of 1,1,1,5,5,5-hexafluoroacetylacetone in 20 mL of MeOH solution containing 0.14 g (0.48 mmol) NaOH. To the yellow solution was added 0.12 g (0.96 mmol) of anhydrous $FeCl_2$. The solution was stirred for 1 h after which the purple precipitate was removed by filtration, washed with H_2O, and dried overnight over P_2O_5. All other metal hexafluoroacetylacetonate $M(hfac)_2$ complexes were obtained from Aldrich as hydrates and stored over P_2O_5 under vacuum. All chemicals used were reagent grade.

† Presented in part at the 211th American Chemical Society National Meeting, New Orleans, LA, March 24−28, 1996.

(1) Breuer, E.; Aurich, H. G.; Nielsen, A. *Nitrones, Nitronates, and Nitroxides*; John Wiley & Sons: New York, 1989.
(2) Torsell, K. B. G. *Nitrile Oxide, Nitrones, and Nitronates in Organic Synthesis*; VCH Publishers: New York, 1988.
(3) Janzen, E. G. *Methods in Enzymology*; Academic Press: Orlando, FL, 1984; Vol. 105, pp 188−198.
(4) Caneschi, A.; Gatteschi, D.; Sessoli, R. *In Molecular Magnetic Materials*; Gatteschi, D., Kahn, O., Miller, J. S., Palacio, F., Eds.; Kluwer Academic Publishers: Dordrecht, The Netherlands, 1991; pp 215−232.
(5) Caneschi, A.; Gatteschi, D.; Rey, P. *Prog. Inorg. Chem.* **1991**, *39*, 331.
(6) Rey, P.; Laugier, J.; Caneschi, A.; Gatteschi, D. *Mol. Cryst. Liq. Cryst.* **1989**, *176*, 337.
(7) Hutchison, J. R.; La Mar, G. N.; Horrocks, W. D. *Inorg. Chem.* **1969**, *8*, 126.
(8) Kluiber, R. W.; Horrocks, W. D. *Inorg. Chim. Acta* **1970**, *4*, 183.
(9) Sivasubramanian, S.; Manisankar, P.; Palaniandavar, M.; Arumagam, N. *Trans. Met. Chem.* **1982**, *7*, 346.
(10) Paulraj, K.; Ramalingam, S. K. *Indian J. Phys.* **1984**, *58B*, 319.
(11) Handwerker, B. M.; Garrett, K. E.; Nagle, K. L.; Geoffreoy, G. L.; Rheingold, A. L. *Organometallics* **1990**, *9*, 1562.
(12) Hutton, A. T.; McEwan, D. M.; Shaw, B. L.; Wilkinson, S. W. *J. Chem. Soc., Dalton Trans.* **1983**, 2011.
(13) Castel, A.; Riviere, P.; Satge, J.; Ahbala, M. *J. Organomet. Chem.* **1986**, *307*, 205.
(14) Keller, H. J.; Leichtert, I.; Uhlmann, G.; Weiss, J. *Chem Ber.* **1977**, *110*, 1684.
(15) Arasasingham, R. D.; Balch, A. L.; Olmstead, M. M.; Renner, M. W. *Inorg. Chem.* **1987**, *26*, 3562.

S0020-1669(97)00974-9 CCC: $15.00
Published on Web 03/17/1998

Instrumentation. ^{1}H HAIR spectra of all complexes were taken on a Nicolet 270 MHz spectrometer in $CDCl_3$ (Aldrich) solutions unless otherwise indicated. Chemical shifts are reported in ppm relative to tetramethylsilane. ^{19}F NMR spectra were obtained on a Bruker (Aspect 3000) 300 MHz spectrometer using a ^{19}F operating frequency of 282.4 Mhz, and chemical shifts were relative to $CFCl_3$. Infrared spectra were recorded on a MIDAC FTIR as KBr pellets, Nujol mulls, thin films on NaCI, and CH_2Cl_2 solutions. UV−vis spectra were taken on a Hewlett-Packard 8451A spectrophotometer, and near-IR spectra on a Hitachi μ-3501 spectrophotometer as CH_2Cl_2 solutions. Microanalytical determinations were done by National Chemical Consulting, Inc.

2-PyBN. Oxidation of 2-(*tert*-butylaminomethyl)pyridine with Na_2WO_4 and H_2O_2 gave 2-PyBN.[16,17] Recrystallization from petroleum ether gave crystals suitable for X-ray analysis.

Complexes with 2-PyBN. To a stirred solution of M(hfac)$_2$ (4.0 mmol) in methylene chloride (30 mL) was added 2-PyBN (0.71 g, 4.0 mmol). Crystals that formed during standing were collected, washed with *n*-heptane, and redissolved in 30 mL of methylene chloride containing 5 mL of toluene. The solution was allowed to evaporate overnight in a desiccator. Single crystals were obtained suitable for X-ray analysis with a typical yield ca. 98%. Analytical, physical, and spectroscopic data for **1**−**5** are given in Table 1.

Complexes with M_3PO. To a stirred suspension of M(hfac)$_2$ (4.0 mmol) in 20 mL of methylene chloride and 5 mL of heptane was added 0.51 g (4.0 mmol) of M_3PO.[18,19] After reflux for 30 min, the solution was filtered and allowed to evaporate slowly at room temperature. Recrystallization from methylene chloride−toluene yielded crystals suitable for X-ray analysis. Analytical, physical, and spectroscopic data for **6**−**9** are given in Table 1.

Preparation of Zn(2-PyPhBN)(hfac)$_2$ (10). Complex **10** was isolated as a decomposition product from a solution of a nitroxide, *N*-oxy-*N*-*tert*-butyl(2-pyridyl)phenylmethanamine (2-PyBNO) and Zn(hfac)$_2$. The 2-PyBNO nitroxide was prepared by addition of 6.0 mL (18.0 mmol) of 3.0 M ether solution of phenylmagnesium bromide (Aldrich) to a stirred solution of 1.52 g (8.53 mmol) of *N*-*tert*-butyl-α-(2-pyridyl)nitrone (2-PyBN) in 100 mL of anhydrous ether at 0 °C under nitrogen. The solution was refluxed for 1 h, after which 50 mL of saturated solution of NH_4Cl was added slowly. The ether layer was separated, and the aqueous layer was washed 3× with 50 mL of ether. The combined extracts were passed through K_2CO_3 and concentrated *in vacuo*. Evaporation of solvent afforded the hydroxylamine as yellow crystals without further recrystallization, 2.00 g (92%). The hydroxylamine (0.1 g, 0.39 mmol) was dissolved in 1 mL of anhydrous ether with freshly prepared Ag_2O (0.18 g, 0.72 mmol) at −5 °C. A silver mirror began to cover the wall of the beaker, and the solution was stirred for additional 1 min at room temperature. The solvent was evaporated under a stream of nitrogen, and then 10 mL of CH_2Cl_2 and 2 mL of heptane were added to the residue. Zn(hfac)$_2$ was added. After 24 h at 5 °C, a black insoluble material formed and the solution was filtered. The yellow filtrate was allowed to stand at room temperature. Colorless crystals separated and were collected for X-ray analysis, yield 0.13 g (45%). Anal. Calcd for $ZnC_{26}H_{21}N_2F_{12}O_5$: C, 42.49; H, 2.88; N, 3.81. Found: C, 42.26; H, 2.30; N, 3.76.

X-ray Crystallographic Determinations. Experimental parameters and crystal data for 2-PyBN and **1**−**5** are presented in Table 2 and for **6**−**10** in Table 3. For **1**−**8** selected crystals were mounted on glass fibers and placed on a Siemens P4 four-circle diffractometer equipped with a rotating Mo anode. Procedures for finding initial reflections, calculation of unit cell parameters, data collection, and data reduction have been described.[20] The wavelength used was 0.710 73 Å. Data collection was performed at 173(2) K except for **2** which was at 295(3) K.

Chart 1. Complexes of 2-PyBN

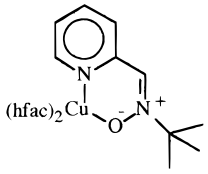

1

$M(2\text{-PyBN})_2(hfac)^+$ $M(hfac)_3^-$

M = Mn(II), **2**

Co(II), **3**

Ni(II), **4**

Fe(II), **5**

The SHELX package of software was used to solve and refine the structures.[21] Direct methods solutions were successful in all cases. Hydrogen atoms were refined isotropically in calculated or observed positions except for **2**, **3**, and **9** in which a riding model was used for calculated positions. Refinements were full-matrix least-squares on F^2 using all data. No corrections for absorption or extinction were applied for **1**−**8**. The weighting scheme used throughout was $w = 1/[\sigma^2(F_o^2) + (AP)^2 + (BP)]$, where $P = (F_o^2 + 2F_c^2)/3$. In all structures problems typical of CF_3 groups were seen, including residual electron density near the fluorine atoms, large fluorine anisotropic thermal parameters, and high correlations between these parameters. However, except where noted below, no convincing disorder models were found. For **2** and **6**−**8** the C−F distances within each CF_3 group were restrained to be equal with a standard deviation of 0.01 Å. Cobalt, nickel, and iron salts were refined as racemic twins. An absolute structure parameter[22] was refined and in both cases the final value of this parameter was indistinguishable from 50% which is consistent with an approximate 50−50 mixture of two lattices.

For 2-PyBN, **9**, and **10** data were taken on a Siemens SMART CCD single-crystal diffractometer with a Mo anode and graphite monochromator (wavelength = 0.710 73 Å). Crystals were mounted on a glass fiber and placed in a nitrogen stream at 173(2) K. A Mo anode and graphite monochromator (wavelength = 0.710 73 Å) were used. A sphere of data was collected out to an effective 2θ value of 55°, using ω scans. Routine Lorentz and polarization corrections were applied. An empirical correction was used[23] for absorption and other systematic errors, based on measured intensities of equivalent reflections at different phi and ω values. Both structures were solved by direct methods. Refinement was full-matrix least-squares against F^2 over all reflections. The programs used were Siemens SMART, SAINT, and SHELXTL.[21,24]

Results and Discussion

X-ray Structures of Bidentate 2-PyBN Complexes. Two fundamentally different structures were observed for M(hfac)$_2$ complexes with 2-PyBN as indicated in Chart 1. The Cu complex **1** which crystallized from an equimolar solution of 2-PyBN and Cu(hfac)$_2$ in CH_2Cl_2 consists of discrete *neutral* Cu(2-PyBN)(hfac)$_2$ units as shown in Figure 1. The coordination geometry is distorted octahedral with two trans Cu−O

(16) Bannett, E. H.; Bronn, W. R.; Coyne, W. E. *J. Med. Chem.* **1977**, *20*, 821.
(17) Murahashi, S.-I.; Mitsui, H.; Shiota, T.; Tanda, T.; Watanabe, S. *J. Org. Chem.* **1990**, *55*, 1736.
(18) Nishi, M.; Hagi, A.; Ide, H.; Murakami, A.; Makino, K. *Biochem. Int.* **1992**, *27*, 651.
(19) Ohkuma, T.; Kirino, Y.; Kwan, T. *Chem. Pharm. Bull.* **1981**, *29*, 25.
(20) *XSCANS User's Manual*, Version 2.18a; Siemens Analytical X-ray Instruments, Inc.: Madison, WI, 1994.
(21) Sheldrick, G. M. *SHELXTL Structure Determination Software Programs*; Siemens Analytical X-ray Instruments, Inc.: Madison, WI, 1990.
(22) (a) Flack, H. D. *Acta Crystallogr.* **1983**, *A39*, 876. (b) Bernardinelli, G.; Flack, H. D. *Acta Crystallogr.* **1985**, *A41*, 500.
(23) Blessing, R. *Acta Crystallogr.* **1995**, *A51*, 33.
(24) (a) Sheldrick, G. M. *Acta Crystallogr.* **1990**, *A46*, 467. (b) *SAINT Users Manual*, Version 4.050; Siemens Analytical X-ray Instruments, Inc.: Madison, WI, 1996.

Table 1. Analytical, Physical, and Spectroscopic Data for **1**−**9**

compd	mp, °C color	anal. %[a]			UV, VIS, near-IR[b]		IR[c]	NMR[d]
		C	H	N	conc, mM	λ_{max}, nm ($\epsilon/10^3$)	λ_{max}, cm^{-1}	δ, ppm
1	146−147 green	36.38 (36.62)	2.14 (2.46)	4.19 (4.27)	0.0090 2.96	232 (19), 308 (27) 765 (0.061), 1245 (1.3)	1657 s, 1609 m, 1551 s 1527 s, 1503 s, 1261 vs, 1150 vs	5.04 (br, 1H), 4.29 (br, 9H) 19.38 (br, 1H)
2	137−138 deep red	37.61 (37.11)	2.23 (2.49)	4.57 (4.33)	0.031	232 (23), 306 (70), 328 (sh)	1647 s, 1605 m, 1556 m, 1532 s, 1506 s, 1255 vs, 1201 vs, 1150 vs	
3	171−172 dk orange	37.31 (36.88)	2.36 (2.48)	4.23 (4.30)	0.012 51.5	230 (25), 304 (65) 540 (sh), 1105 (0.011)	1643 s, 1526 m, 1507 m 1259 vs, 1200 s, 1147 vs	24.36 (s, 9H), −14.35 (s, 1H), −22.04 (s, 2H), 6.71 (s, IH), 10.06 (s, 1H), 42.36 (s,1H), 71.28 (s, 1H)
4	178−180 dk green	38.48 (36.89)	2.39 (2.48)	4.32 (4.30)	0.0060 88.9	230 (40), 268 (38), 316 (69) 626 (21), 1038 (18)	1647 vs, 1552 m, 1523 s, 1506 s, 1261 vs, 1209 vs 1147 vs	5.05 (br, 9H), −10.95 (br, 1H), −9.10 (br, 1H), −48.90 (s, 1H), 21.4 (br, 1H), 29.45 (br, 1H), 36.90 (br, 1H) ^{19}F NMR −24.29 (br, 1F), −26.95 (br, 1F), −27.63 (br, 1F), −29.98 (br, 1F)
5	145−147 purple	37.11 (37.06)	2.55 (2.49)	4.38 (4.32)	0.031	232 (17), 306 (41), 396 (1.7), 564 (2.0)	1629 m, 1497 m, l260 vs, 1207 vs, 1145 vs	−64.0 (br, 1H), −8.24 (br, 1H), −0.46 (br, 4H), 1.77 (br, 9H), 10.81 (br, 1H), 25.4 (br, 1H), 34.95 (br, 1H)
6	187−190 yellow	34.31 (34.24)	2.15 (2.54)	2.41 (2.35)	0.0040	230 (41), 304 (46), 330 (sh)	1644 vs, 1556 s, 1530 s, 1506 s, 1257 vs, 1211 vs, 1148 vs	
7	195−197 dk red	34.06 (34.01)	2.25 (2.52)	2.33 (2.33)	0.0030 2.51	230 (41), 304 (46) 582 (0.18), 846 (0.020)	1649 s, 1554 m, 1529 m 1507 m, 1261 vs, 1212 vs, 1148 vs	
8	210−220 (d) green	34.86 (34.03)	2.24 (2.52)	2.28 (2.34)	0.011 2.52	232 (23), 316 (34) 6.84 (0.025), 1198 (0.024)	1649 s, 1557 m, 1528 m 1508 m, 1269 vs, 1208 vs, 1145 vs	
9	124−125 red	33.81 (33.30)	2.16 (2.47)	2.36 (2.28)	0.050	240 (29), 278 (28), 360 (12), 482 (1.0)	1649 s, 1557 m, 1529 m, 1480 s, 1259 vs, 1213 vs, 1150 vs, 838 m	

[a] Calculated values in parentheses. [b] In CH_2Cl_2. [c] As KBr pellet. [d] In $CDCl_3$ with internal TMS; ^{1}H NMR unless otherwise indicated.

Table 2. Crystallographic Data for 2-PyBN and **1**−**5**

compound	2-PyBN	**1**	**2**	**3**	**4**	**5**
chemical formula	$C_{10}H_{14}N_2O$	$CuC_{20}H_{16}F_{12}N_2O_5$	$Mn_2C_{40}H_{32}F_{24}N_4O_{10}$	$Co_2C_{40}H_{22}F_{24}N_4O_{10}$	$Ni_2C_{40}H_{32}F_{24}N_4O_{10}$	$Fe_2C_{40}H_{32}F_{24}N_4O_{10}$
fw	178.23	655.89	1294.58	1302.56	1302.12	1296.40
space group, *Z*	$Pca2_1$ (No. 29), 4	$P2_1/c$ (No. 14), 8	$C2/c$ (No. 15), 4	$P2_12_12$ (No. 18), 2	$P3_121$ (No. 152), 3	$P3_121$ (No. 152), 3
a (Å)	11.9992(7)	16.716(4)	17.106(3)	8.486(3)	11.330(1)	11.372(4)
b (Å)	8.7696(5)	14.222(6)	21.500(2)	15.988(4)	11.330(1)	11.372(4)
c (Å)	9.6030(5)	22.689(5)	15.863(2)	18.959(4)	34.643(6)	34.649(2)
α (deg)	90	90	90	90	90	90
β (deg)	90	109.76(1)	112.32(1)	90	90	90
γ (deg)	90	90	90	90	120	120
unit cell volume (Å^3)	1010.51(10)	5076(3)	5397.0(13)	2572.2(123	3851.3(8)	3880.2(3)
ρ_{calc} (g cm^{-3})	1.172	1.716	1.593	1.682	1.684	1.664
μ (cm^{-1})	0.77	9.83	6.05	7.88	8.77	7.04
T (°C)	−100	−100	20	−100	−100	−100
final *R*[a]	$R_1 = 0.0328$, $wR_2 = 0.0813$	$R_1 = 0.068$, $wR_2 = 0.124$	$R_1 = 0.086$, $wR_2 = 0.242$	$R_1 = 0.074$, $wR_2 = 0.170$	$R_1 = 0.047$, $wR_2 = 0.106$	$R_1 = 0.086$, $wR_2 = 0.176$

[a] $R_1 = \sum||F_o| - |F_c||/\sum|F_o|$ with $I > 2\sigma(I)$ and $wR_2 = [\sum[w(F_o^2 - F_c^2)^2]/\sum[w(F_o^2)^2]]^{1/2}$.

Table 3. Crystallographic Data for **6**−**10**

compound	**6**	**7**	**8**	**9**	**10**
empirical formula	$Mn_2C_{34}H_{30}F_{24}N_2O_{10}$	$Co_2C_{34}H_{30}F_{24}N_2O_{10}$	$Ni_2C_{34}H_{30}F_{24}N_2O_{10}$	$Fe_2C_{34}H_{30}F_{24}N_2O_{10}$	$ZnC_{26}H_{20}F_{12}N_2O_5$
fw	l192.48	1200.46	1200.02	1210.30	733.81
space group, *Z*	$C2/c$ (No. 15), 4	$C2/c$ (No. 15), 4	$C2/c$ (No. 15), 4	$P\bar{1}$ (No. 2), 2	$P2_1/n$ (No. 14), 4
a (Å)	9.659(3)	10.152(2)	10.242(2)	11.8441(6)	15.0257(8)
b (Å)	26.362(3)	25.223(2)	25.004(3)	12.8891(6)	12.7111(6)
c (Å)	18.942(2)	18.655(2)	18.601(2)	18.0199(9)	16.3713(8)
α (deg)	90	90	90	78.002(1)	90
β (deg)	97.46(2)	98.20(1)	97.72(1)	76.711(1)	110.725(1)
γ (deg)	90	90	90	63.038(1)	90
unit cell volume (Å^3)	4782(2)	4728(1)	4721(1)	2369.2(2)	2924.6(3)
ρ_{calc} (g cm^{-3})	1.656	1.686	1.688	1.697	1.667
μ (cm^{-1})	6.73	8.49	9.45	7.62	9.56
T (°C)	−100	−100	−100	−150	−100
final *R*[a]	$R_1 = 0.087$, $wR_2 = 0.231$	$R_1 = 0.083$, $wR_2 = 0.203$	$R_1 = 0.080$, $wR_2 = 0.178$	$R_1 = 0.086$, $wR_2 = 0.220$	$R_1 = 0.048$, $wR_2 = 0.091$

[a] $R_1 = \sum||F_o| - |F_c||/\sum|F_o|$ with $I > 2\sigma(I)$ and $wR_2 = [\sum[w(F_o^2 - F_c^2)^2]/\sum[w(F_o^2)^2]]^{1/2}$.

bonds elongated. There are two independent molecules in the asymmetric unit, each having a different pair of elongated bonds. In one, hfac oxygen O3 and a nitrone oxygen O1 are axial (Figure 1a); in the other, oxygens from two different hfac ligands are axial (Figure 1b). Table 4 summarizes the copper coordination geometry of the two independent molecules in the asymmetric unit.

In contrast to **1** the solid state structures of **2**−**5** are *complex salts* consisting of M(2-PyBN)$_2$(hfac) cations and M(hfac)$_3$ anions (Figure 2), all having approximately octahedral coordination. Bond distances and angles for the metal coordination sphere for these complexes are given in Table 5. Surprisingly, three different space groups were found for this series of similar salts, with **4** and **5** falling in the same space group. However, in every case the metal atoms of both ions fall on crystallographic 2-fold rotation axes which also pass through the C−H bond of a hfac ligand. There also is evidence that at least one compound crystallizes in two space groups. One sample of **3** was observed in the trigonal space group $P3_121$ (also observed for **4** and **5**). A structure based on an incomplete data set[25] was refined to $R_1 = 0.135$ and exhibited the general features of the other complex salts. A second complete data set was collected using a crystal obtained from a second sample, and this structure, with space group $P2_12_12$, is the one reported in this paper. Although crystallization conditions were similar for both cobalt samples, a different crystalline habit and space group were observed for the second sample.

The formation of complex salts rather than neutral complexes for these compounds is surprising in view of the structures reported for the M(hfac)$_2$ derivatives of the nitronyl nitroxide pyridine ligand 2-(2-pyridyl)-4,4,5,5-tetramethyl-4,5-dihydro-1H-imidazolyl-1-oxy 3-oxide (NIT2-Py).[26] The NIT2-Py complexes of Mn(II) and Ni(II) are analogous to **1**, in that neutral complexes are formed rather than complex salts. To our knowledge, there has been no similar ligand exchange observed for M(hfac)$_2$ with any bidentate ligands. Neutral complexes usually result from such mixtures.

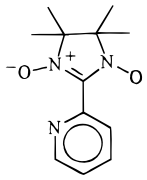

NIT2-Py

Geometry of the 2-PyBN Ligand. The free ligand, shown in Figure 3, has a nitrone N−O bond length of 1.2935(13) Å

(25) Crystallographic data for [Co(2-PyBN)$_2$(hfac)][Co(hfac)$_3$]: trigonal, $P3_221$, $a = 11.533(1)$ Å, $c = 35.207(4)$ Å, $V = 4055.5(7)$ Å^3, $T = 293(2)$ K, $Z = 3$, absolute structure parameter = 0.2(1), 303 parameters, 4068 independent reflections. All non-hydrogen atoms were located and refined. Some atoms could be refined anisotropically, but attempts to refine all non-hydrogen atoms anisotropically failed. Nearly 2000 data were missing from a $2\theta = 55°$ data set due to diffractometer malfunction.

(26) Luneau, D.; Risoan, G.; Rey, P.; Grand, A.; Caneschi, A.; Gatteschi, D.; Laugier, J. *Inorg. Chem.* **1993**, *32*, 5616.

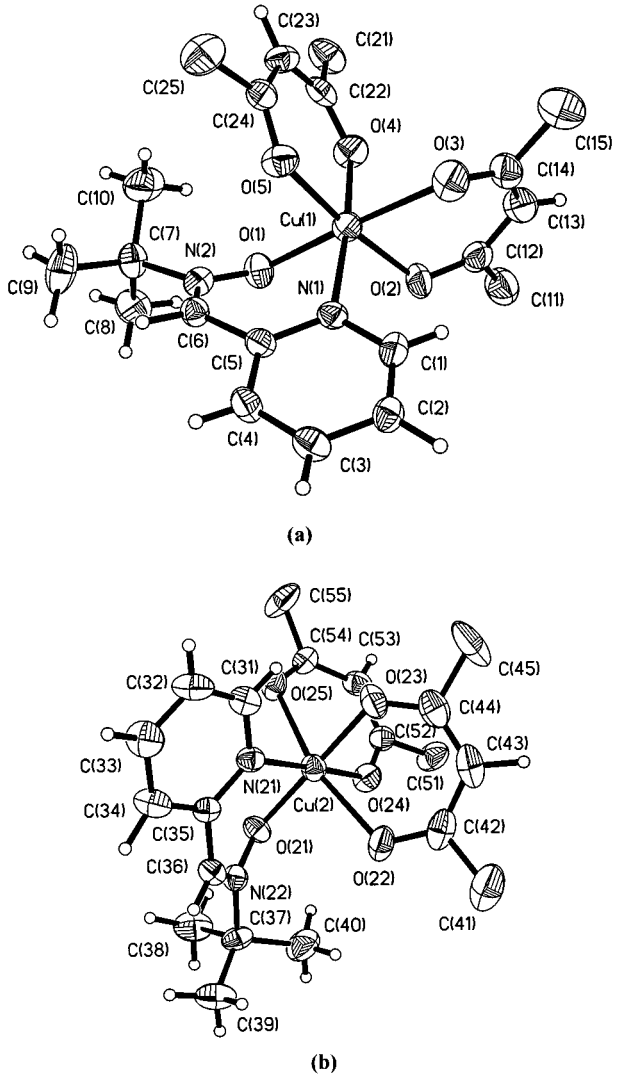

Figure 1. Views of the two independent Cu(2-PyBN)(hfac)$_2$, **1**, molecules in the asymmetric unit showing the numbering scheme. Displacement ellipsoids are drawn at 50% probability. Fluorine atoms have been omitted for clarity, and hydrogen atoms are represented as circles of arbitrary radius.

and C═N length of 1.307(2) Å. On complexation, the pyridyl ring rotates by nearly 180° bringing the pyridyl nitrogen and nitrone oxygen into a syn relationship. The N−O bond lengthened slightly for **1**−**5**, while C═N shortened. These changes, however, were statistically significant only for N−O lengthening of **3** and **5** and C═N shortening for **1**−**3** and **5**. A larger change was an increase in dihedral angle between pyridine and C═NO planes from 11.62(10)° for 2-PyBN to 28.0(4) and 25.3(3)° for the two independent molecules of **1**, and to 14.5(5), 18.6(4), 21.7(3), and 21.7(4)° for **2**, **3**, **4**, and **5**, respectively.

Two effects can explain N−O lengthening and C═N shortening: (i) coordination to a metal ion increases the importance of resonance form I with a C═N and (ii) increased nonplanarity of the pyridine and nitrone functions reduces delocalization of electrons from O into the pyridine ring, and hence the importance of delocalized form II.

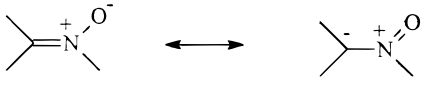

I II

The N−M−O "bite" angle defined by the pyridine nitrogen, the metal, and the nitrone oxygen (Nl, Ml, O1 in Tables 4 and 5), also changes with the metal atom. The observed trends correlate with the decrease in ionic radius in going from Mn(II) to Cu(II). The only exception is the N−M−O angle on the particular copper complex in which the nitrone oxygen is an axial ligand and therefore has a longer M−O distance due to the axial distortion found for copper.

Table 4. Distances (Å) and Angles (deg) for Cu Coordination Sphere in **1**

Cu1−O1	2.130(4)	Cu2−O21	1.944(4)
Cu1−N1	1.989(5)	Cu2−N21	1.989(5)
Cu1−O2	2.079(5)	Cu2−O22	2.274(5)
Cu1−O3	2.198(5)	Cu2−O23	1.977(4)
Cu1−O4	1.930(4)	Cu2−O24	1.969(4)
Cu1−O5	2.058(5)	Cu2−O25	2.269(5)
O4−Cu1−N1	173.4(2)	O21−Cu2−O24	179.2(2)
O4−Cu1−O5	91.3(2)	O21−Cu2−O23	88.4(2)
N1−Cu1−O5	89.0(2)	O24−Cu2−O23	91.2(2)
O4−Cu1−O2	86.9(2)	O21−Cu2−N21	88.3(2)
N1−Cu1−O2	93.5(2)	O24−Cu2−N21	92.1(2)
O5−Cu1−O2	173.9(2)	O23−Cu2−N21	176.6(2)
O4−Cu1−O1	88.7(2)	O21−Cu2−O25	94.8(2)
N1−Cu1−O1	84.7(2)	O24−Cu2−O25	85.9(2)
O5−Cu1−O1	94.3(2)	O23−Cu2−O25	84.7(2)
O2−Cu1−O1	91.5(2)	N21−Cu2−O25	96.6(2)
O4−Cu1−O3	89.7(2)	O21−Cu2−O22	96.1(2)
N1−Cu1−O3	96.9(2)	O24−Cu2−O22	83.2(2)
O5−Cu1−O3	90.1(2)	O23−Cu2−O22	85.2(2)
O2−Cu1−O3	84.1(2)	N21−Cu2−O22	94.1(2)
O1−Cu1−O3	175.3(2)	O25−Cu2−O22	165.0(2)
C1−N1−Cu1	120.5(4)	C31−N21−Cu2	120.4(5)
C5−N1−Cu1	121.5(4)	C35−N21−Cu2	122.0(4)
N2−O1−Cu1	114.4(4)	N22−O21−Cu2	118.4(4)
C12−O2−Cu1	124.1(5)	C42−O22−Cu2	120.1(4)
C14−O3−Cu1	121.0(5)	C44−O23−Cu2	128.0(4)
C22−O4−Cu1	126.3(4)	C52−O24−Cu2	125.3(5)
C24−O5−Cu1	123.0(4)	C54−O25−Cu2	117.1(5)

X-ray Structures of Monodentate M_3PO Complexes. Attempts to make M(M_3PO)$_2$(hfac)$_2$ complexes from 2:1 ratios of M_3PO with M(hfac)$_2$ were unsuccessful, as the final reaction mixture always contained unreacted M_3PO. However, an equimolar mixture produced 1:1 complexes with crystals suitable for X-ray analysis. This isostructural series of *dimeric* derivatives has the formula [M(M_3PO)(hfac)$_2$]$_2$, where M = Mn, CO, or Ni, as indicated in Chart 2. The neutral molecules consist of two M(hfac)$_2$ units bridged by oxygen atoms of two different M_3PO ligands in a bis-μ-1,1 fashion, as shown in Figure 4. Each metal has a distorted octahedral coordination geometry, with all angles within 17° of 90 and 180°, with the exception of an angle of 156(2)° for O4−Mn−O4′ in 6. Each pair of dimer metal atoms lies on a crystallographic 2-fold axis. The metal−metal distances in **6**−**8** are 3.491(2), 3.337(1), and 3.295(2) Å, respectively.

The overall structure is similar to that reported for the Mn(hfac)$_2$ dimer of 2-phen,4,4,5,5-tetramethylimidazoline 3-oxide (AmPh),[27] as well as a series of nitronyl nitroxide structures

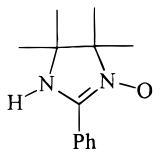

AmPh

containing Mn(II) or Co(II).[28−30] Analogous structures have

(27) Carducci, M. D.; Doedens, R. J. *Inorg. Chem.* **1989**, *28*, 2492.

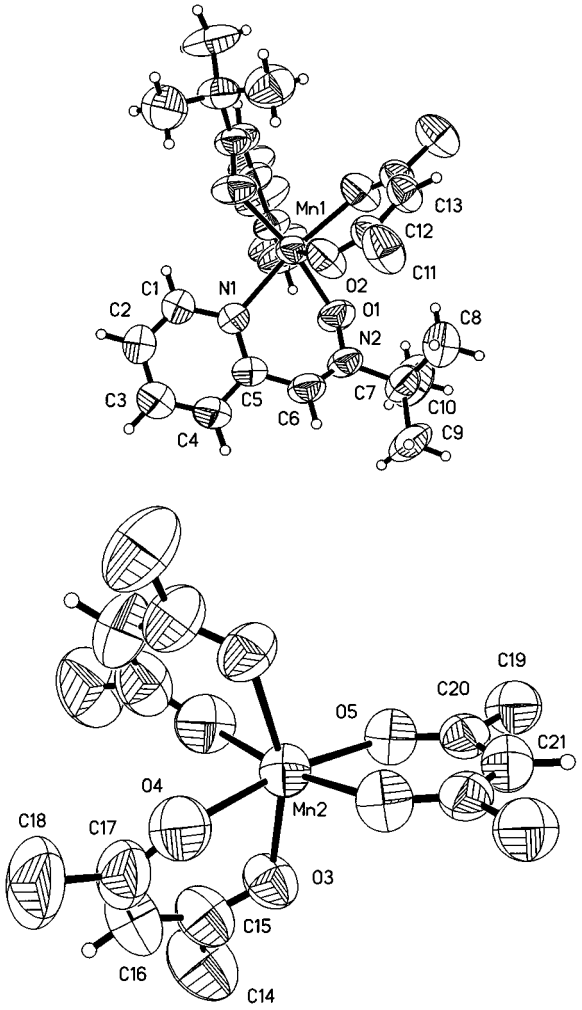

Figure 2. View of **2** showing the numbering scheme for $[M(2\text{-PyBN})_2(hfac)]^+$ cations (top) and $[M(hfac)_3]^-$ anions of **2**−**5**. Displacement ellipsoids are drawn at 50% probability. Fluorine atoms have been omitted for clarity, and hydrogen atoms are represented as circles of arbitrary radius.

also been observed for pyridine oxide complexes of copper,[31,32] cobalt,[33] cadmium,[34] siIver,[35] and zinc[36] and for hydroxylamine complexes of molybdenum[37] and tungsten.[38]

X-ray analysis of the crystals obtained from CH_2Cl_2 solutions containing M_3PO and $Fe(hfac)_2$ revealed an entirely different structure. An apparent air oxidation of starting $Fe(hfac)_2$ led to the (μ-oxo)diiron(III) complex $[Fe(M_3PO)(hfac)_2]_2$ (μ-O) (**9**)

(28) Caneschi, A.; Gatteschi, D.; Laugier, J.; Rey, P.; Sessoli, R. *Inorg. Chem.* **1988**, *27*, 1553.
(29) Caneschi, A.; Gatteschi, D.; Laugier, J.; Rey, P.; Zanchini, C. *Inorg. Chem.* **1989**, *28*, 1969.
(30) Benelli, C.; Caneschi, A.; Gatteschi, D.; Melandri, M. C. *Inorg. Chim. Acta* **1990**, *172*, 137.
(31) Baran, P., Koman, M., Valigura, D., Mrozinski, J. *J. Chem. Soc., Dalton Trans.* 1991, 1385.
(32) Melnik, M. *Coord. Chem. Rev.* **1982**, *42*, 259.
(33) Craig, D. C.; Phillips, D. J.; Kaifi, F. M. Z. *Inorg. Chim. Acta* **1989**, *161*, 247.
(34) Nieuwenhuyzen, M.; Robinson, R.; Wilkins, C. J. *Polyhedron* **1991**, *10*, 2111.
(35) Bagieu-Beucher, M.; Le Fur, Y.; Levy, J.-P.; Pecaut, J. *Acta Crystallogr.* **1994**, *C50*, 1079.
(36) Barnett, B. L.; Kretschmar, H. C.; Hartman, F. A. *Inorg. Chem.* **1977**, *16*, 1834.
(37) Wieghardt, K.; Holzbach, W.; Hofer, E.; Weiss, J. *Chem. Ber.* **1981**, *114*, 2700.
(38) Redshaw, C; Wilkinson, G, Hussain-Bates, B., Hursthouse, M. B. *J. Chem. Soc., Dalton Trans.* 1992, 555.

Table 5. Bond Distances (Å) and Angles (deg) for Metal Coordination Sphere in **2**−**5**[a]

atoms	**2**	**3**	**4**	**5**
M1−O1	2.095(4)	2.025(5)	2.027(2)	2.069(4)
M1−N1	2.248(5)	2.113(5)	2.059(3)	2.178(5)
M1−O2	2.178(4)	2.075(5)	2.029(3)	2.056(5)
M2−O5	2.155(4)	2.042(5)	2.023(3)	2.095(4)
M2−O3	2.161(5)	2.055(5)	2.028(3)	2.087(4)
M2−O4	2.163(5)	2.066(5)	2.031(3)	2.072(4)
O1−M1−O1′	167.2(3)	175.1(3)	179.7(14)	171.9(3)
O1−M1−O2′	95.4(2)	90.6(2)	90.6(11)	92.7(2)
O1−M1−O2	94.2(2)	92.9(2)	89.6(11)	93.2(2)
O2−M1−O2′	82.6(2)	88.1(3)	89.5(2)	87.1(2)
O1−M1−N1	80.6(2)	85.5(2)	85.9(11)	81.7(2)
O2−M1−N1	85.4(2)	86.6(2)	88.4(11)	89.8(2)
O1−M1−N1′	91.7(2)	91.3(2)	93.9(12)	92.7(2)
O2−M1−N1′	167.1(2)	173.3(2)	175.0(12)	173.5(2)
N1−M1−N1′	106.9(3)	99.0(3)	94.1(2)	93.8(3)
O5−M2−O5′	82.2(2)	88.2(3)	92.8(2)	88.4(2)
O5−M2−O3	92.3(2)	89.4(2)	89.3(11)	88.2(2)
O5−M2−O3′	104.3(2)	92.8(2)	86.9(12)	87.1(2)
O3−M2−O3′	158.0(3)	176.9(3)	174.5(2)	173.4(3)
O5−M2−O4′	170.4(2)	177.6(2)	175.1(12)	172.6(2)
O5−M2−O4	92.3(2)	93.0(2)	91.3(11)	94.1(2)
O3−M2−O4	81.4(2)	88.5(2)	90.6(10)	86.0(2)
O3−M2−O4′	83.7(2)	89.2(2)	93.5(12)	98.9(2)
O4−M2−O4′	94.2(3)	85.9(3)	84.6(2)	84.2(3)
N2−O1−M1	124.8(3)	118.8(5)	119.7(2)	121.6(3)
C12−O2−M1	128.7(4)	124.7(5)	125.2(3)	126.9(4)
C15−O3−M2	123.8(5)	124.1(5)	124.0(3)	127.2(4)
C17−O4−M2	125.5(5)	123.3(4)	121.6(3)	124.7(4)
C20−O5−M2	129.8(4)	125.1(5)	122.3(3)	124.6(4)
C5−N1−M1	123.1(4)	121.1(5)	122.3(2)	121.8(4)
C1−N1−M1	119.4(4)	120.4(4)	119.6(3)	118.4(4)

[a] Atoms marked by a prime (′) are generated by the 2-fold axis passing through the metal center.

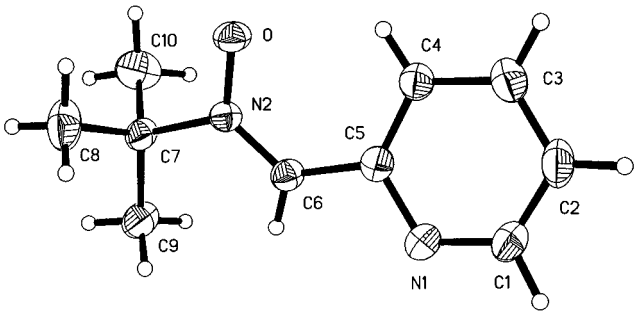

Figure 3. View of 2-PyBN. Displacement ellipsoids are drawn at 50% probability. Hydrogen atoms are represented as circles of arbitrary radius.

shown in Figure 5. One of the M_3PO nitrones was severely disordered, occupying two positions in an approximate 1:1 ratio, and some CF_3 groups also were disordered. The Fe−O(hfac) bonds trans to the oxo group are on average 0.081 Å longer than the cis, resulting in a distorted octahedral coordination geometry for the iron. The $Fe-O_{oxo}$ bond lengths are 1.779(3) and 1.780(3) Å. For the hfac ligands, $Fe-O_{cis}$ distances range from 2.041 (3) to 2.090(4) Å, and $Fe-O_{trans}$ are 2.138(4) and 2.151(3) Å. The $Fe-O_{nitrone}$ distances are 1.990(4) and 1.999(4) Å. Average N−O and C═N distances in the nitrone are 1.33(2) and 1.26(3) Å, respectively. The average Fe−O−N angle is 127(2)°, and the Fe−O−Fe angle is 150.4(2)°.

Additional evidence consistent with an oxo dimer structure for **9** included an IR absorption at 838 cm^{-1}, a UV−vis peak at 360 nm and a magnetic moment measurement by the Evans method with $\mu_B = 3.5(5)$ indicating antiferromagnetic coupling between the two Fe(III) centers.[39] Structural reports of iron

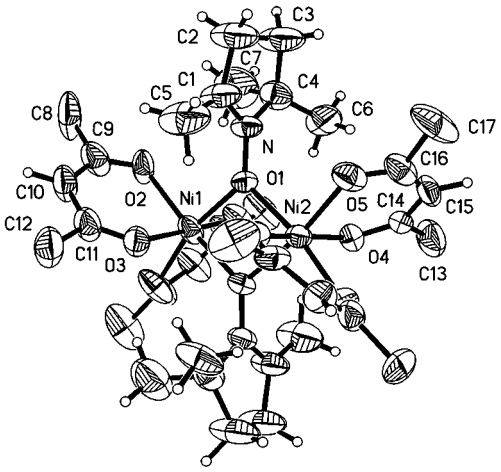

Figure 4. View of **8** showing the numbering scheme for the asymmetric unit of $[M(hfac)_2(M_3PO)]_2$ of **6**−**8**. Displacement ellipsoids are drawn at 50% probability. Fluorine and hydrogen atoms have been omitted for clarity. The hfac rings illustrated are those with the highest occupancy factors. The asymmetric unit shown is for $[Ni(hfac)_2(M_3PO)_2$.

Chart 2. Complexes of M_3PO

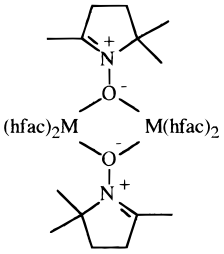

M = Mn(II), **6**

Co(II), **7**

Ni(II), **8**

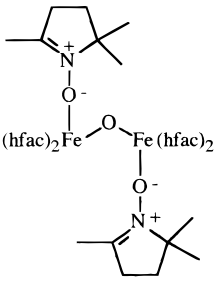

9

μ-oxo dimers with an $O_5-Fe-O-Fe-O_5$ coordination pattern are rare for compounds having organic ligands. The only other examples of which we are aware also arise from oxidation of $Fe(hfac)_2$.[40]

Geometry of the M_3PO Ligand. The M_3PO bond lengths and angles follow the expected pattern with the N−C1 double bond being significantly shorter (by ca. 0.16 Å) than the N−C4 single bond. The average N−O distance of 1.345(1) is slightly shorter than those found for complexes of reduced imidazolyl nitronyl nitroxides,[29,32] in which the N−O distance ranged from 1.366(6) to 1.392(9).

(39) (a) Kurtz, D. M., Jr. *Chem. Rev.* **1990**, *90*, 585. (b) Lippard, S. J. *Angew. Chem., Int. Ed. Engl.* **1988**, *27*, 344.

(40) (a) Ahlers, C.; Dickrnan, M. H. Abstract #677 (Inorganic Division), 211th ACS National Meeting, New Orleans, LA 1996. (b) Dickman, M. H., manuscript in preparation.

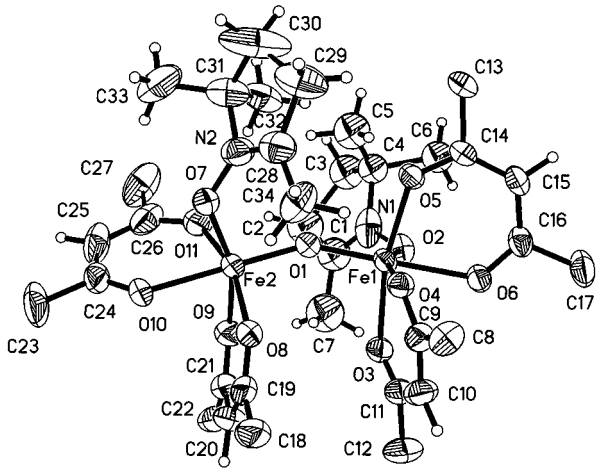

Figure 5. View of $[Fe(M_3PO)(hfac)_2]_2$ (μ-O), **9**. Displacement ellipsoids are drawn at 50% probability. Fluorine atoms and the third (disordered) M_3PO ring have been omitted for clarity, and hydrogen atoms are represented as circles of arbitrary radius.

The five-membered M_3PO ring is approximately in an envelope conformation. The oxygen, nitrogen, and two carbon atoms attached to it (C1 and C4) are coplanar within 0.02 Å; C2 is only about 0.06(2) Å out of this plane, while C3 is about 0.41 (2) Å out of the same plane, displaced in the same direction as C2.

Disorder of the hfac Ligands. During refinement of **6**−**8** it became clear that in each case the hfac ligands were disordered on one or both of the metal atoms in two different ways. The nature of one of the types of disorder can be described in the following manner. Given that two cis-octahedral positions are occupied by the nitrone ligands, there are two isomers possible in which two bidentate hfac ligands could occupy the remaining four sites on a single metal atom. In the present dimers the hfac ligands are disordered on one metal atom such that both of these isomers are superimposed (Figure 6a). This type of disorder is seen on the metal atom labeled M2 in all three structures.

A second type of confirmational disorder was found for one hfac ligand on the other metal atom (M1) in **7** and **8**. This type of disorder appeared as a second hfac ring nearly superimposed on the first but apparently rotated through a small angle around one of the hfac C−O bonds (Figure 6b). Both types of disorder existed, each in about a 65−35% ratio for **7** and **8**, while **6** exhibited only the first type of disorder with a 55−45% ratio.

As a result of this severe disorder the CF_3 groups in **6**−**8** are even less well defined than usual for hfac ligands. As might be expected the final models include high values for fluorine anisotropic displacement parameters with some large (ca. 70%) correlations between these parameters for some fluorine atoms.

Structure of Zn(2-PyPhBN)(hfac)$_2$ 10. An unexpected metal−nitrone complex **10** (Figure 7) was obtained from a mixture containing $Zn(hfac)_2$ and a bidentate nitroxyl radical during an attempt to make a zinc−nitroxyl complex. As shown in Scheme 1, the nitrone 2PyPhBN presumably resulted from disproportionation of β-hydrogen-containing radical **B** formed by oxidation of hydroxylamine **A** with Ag_2O. The Zn atom has a distorted octahedral coordination geometry, with hfac Zn−O distances ranging from 2.068(2) to 2.101(2) Å. The Zn−$O_{nitrone}$ distance is 2.053(2) Å, and the Zn−N distance is 2.130(2)

Scheme 1. Formation of Zn(II) Complex **10**

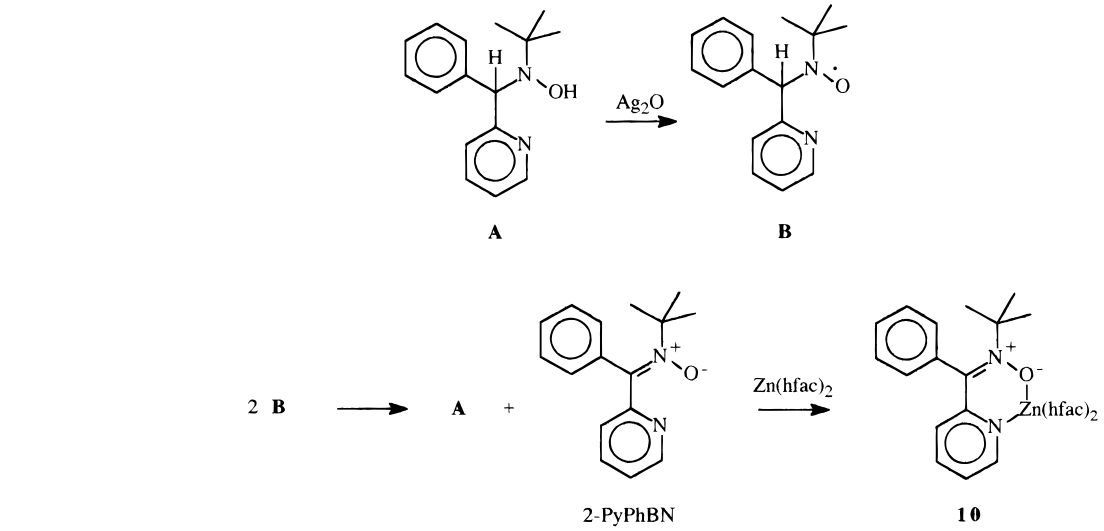

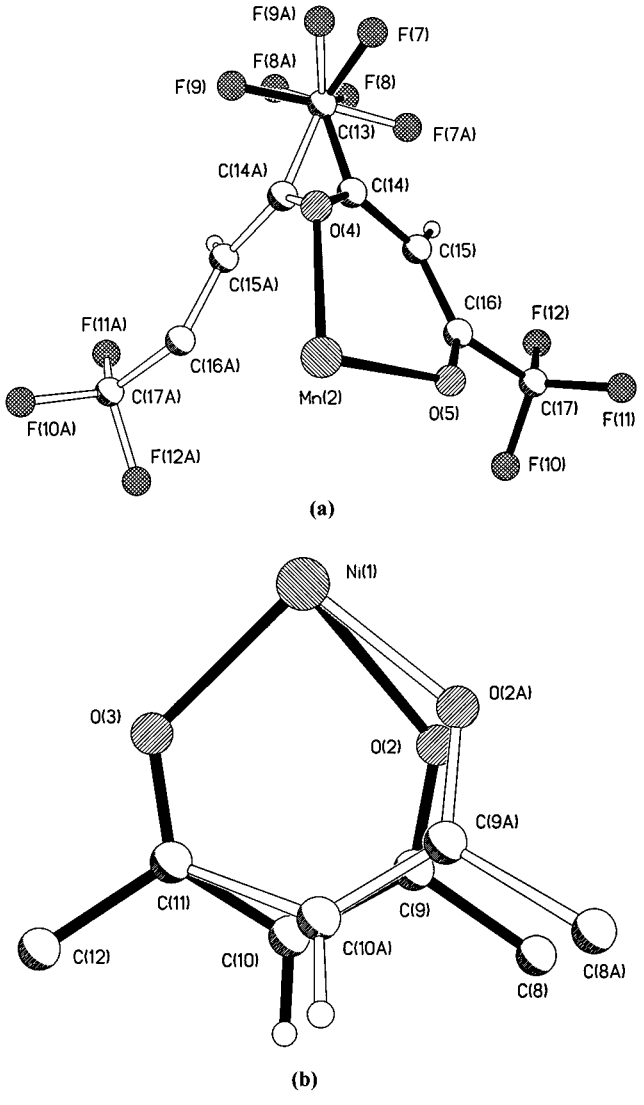

Figure 6. Ball-and-stick diagrams showing the first and second types of disorder found in **6**−**8**. See text for explanation.

Å. The N(2)−O(1) bond distance of 1.324(2) Å is comparable to those of **1**−**5** (1.304(6)−1.325(6) Å), while the N(2)−C(6) bond distance of 1.311(3) Å is only slightly longer (1.26(1)−1.285(5) Å).

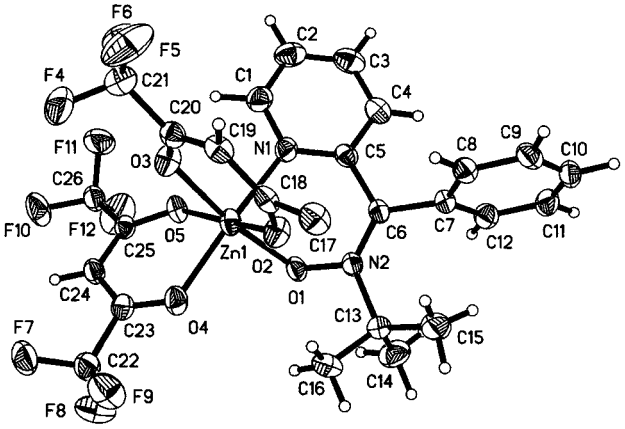

Figure 7. View of Zn(2-PyPhBN)(hfac)$_2$, **10**, showing the numbering scheme. Some fluorine atoms have been omitted for clarity. Displacement ellipsoids are drawn at 50% probability, with hydrogen atoms drawn as circles of arbitrary radius.

Conclusions

The present X-ray results reveal a striking range of behavior of nitrones as ligands. With a bidentate nitrone, Cu forms a neutral complex, while Mn, CO, Ni, and Fe produce crystals with complex salt structures resulting from an unusual ligand exchange with M(hfac)$_2$. The driving force for the formation of the salt from the neutral form by 2-PyBN is unclear but may be due to lower solubility of the ionic crystal form in a nonpolar solvent. Geometry changes in 2-PyBN on complexation indicate a more localized nitrone C═N bond in **1**−**5**. With the monodentate nitrone M_3PO, a third type of crystalline form was obtained in which the nitrone acts as a bridging ligand producing a dimeric complex. With Fe(hfac)$_2$, however, M_3PO gave a (μ-oxo)diiron(III) dimer, presumably by air oxidation of Fe(II). A diamagnetic neutral monomeric complex was obtained from complexation of Zn(hfac)$_2$ with the bidentate 2-PyPhBN.

Acknowledgment. The diffractometer was obtained with the assistance of a grant from the NSF.

Supporting Information Available: Listings of atomic positional parameters, isotropic and anisotropic thermal parameters, hydrogen atom parameters and complete bond distances and angles for 2-PyBN and **1**−**10** (74 pages). Ordering information is given on any current masthead page.

IC9709741